

To appear in *Philosophical Magazine*
Vol. 00, No. 00, Month 20XX, 1–21

Ubiquity of Unconventional Phenomena Associated with Critical Valence Fluctuations in Heavy Fermion Metals

K. Miyake^{a*} and S. Watanabe^b

^a *Toyota Physical and Chemical Research Institute, Nagakute, Aichi 480-1192, Japan;*

^b *Department of Basic Sciences, Kyushu Institute of Technology, Kitakyushu, Fukuoka 804-8550, Japan*

(December 16, 2016)

Ubiquity of unconventional phenomena observed in a series of heavy fermion metals is discussed on the basis of an idea of critical valence fluctuations. After surveying experimental aspects of these unconventional behaviors in prototypical compounds, $\text{CeCu}_2(\text{Si,Ge})_2$, under pressure, we propose that sharp valence crossover phenomena are realized in CeCu_6 , CeRhIn_5 , and $\text{Ce}(\text{Ir,Rh})\text{Si}_3$ by tuning the pressure and the magnetic field simultaneously, on the basis of previous results for an extended Anderson lattice model with the Coulomb repulsion U_{fc} between localized f-electron and itinerant conduction electrons.

Keywords: critical valence fluctuations, unconventional criticality, $\text{CeCu}_2(\text{Si,Ge})_2$, CeCu_6 , CeRhIn_5 , $\text{Ce}(\text{Ir,Rh})\text{Si}_3$

1. Introduction

In the past decade or so, it gradually turned out that the critical-valence-transition or sharp-valence-crossover phenomena in heavy fermion metals is rather ubiquitous than first thought in the beginning of the present century. Indeed, unconventional quantum critical phenomena, which cannot be understood on the basis of the quantum criticality associated with magnetic transitions, have been observed in a series of heavy fermion metals, $\text{YbCu}_{5-x}\text{Al}_x$ ($x=3.5$) [1, 2], YbRh_2Si_2 [3, 4], YbAuCu_4 [5, 6], $\beta\text{-YbAlB}_4$ [7], $\alpha\text{-YbAl}_{1-x}\text{Fe}_x\text{B}_4$ ($x=0.014$) [8], and quasi-crystal compound $\text{Yb}_{15}\text{Al}_{34}\text{Au}_{51}$ [9] and quasi-crystal-approximant $\text{Yb}_{14}\text{Al}_{35}\text{Au}_{51}$ under pressure $P \simeq 1.8\text{GPa}$ as well [10]. The non-Fermi liquid behaviors observed in these compounds can be explained in a coherent way by a scenario based on the critical valence fluctuations (CVF) using the mode-mode coupling approximation for CVF [11, 12], as summarized in Table 1. A recent highlight is that the so-called T/B scaling behavior of the magnetization, observed in $\beta\text{-YbAlB}_4$ [7, 17, 18], and quasi-crystal related compounds $\text{Yb}_{15}\text{Al}_{34}\text{Au}_{51}$ [19] and $\text{Yb}_{14}\text{Al}_{35}\text{Au}_{51}$ [10], has been theoretically derived by taking into account the effect of the magnetic field in the mode-mode coupling approximation scheme [20, 21].

The unconventional phenomena associated with sharp valence crossover have also been observed in a series of Ce-based heavy fermion metals, while the complete

*Corresponding author. Email: miyake@toyotariken.jp

Table 1. Theoretical results for a series of physical quantities by critical valence fluctuations (CVF) giving the exponent ζ as $0.5 \lesssim \zeta \lesssim 0.7$ depending on the region temperature T higher than T_0 , the extremely small temperature scale (see §6 and §7), and unconventional criticality observed in a series of materials. $T^{1.5} \rightarrow T$ in the column $\rho(T)$ means that T dependence of $\rho(T)$ crosses over from $T^{1.5}$ at $T < T_0$ to T at $T > T_0$ around $T \sim T_0$. The symbol * indicates that there is no available experiment. In the last row, theoretical prediction on the conventional criticality associated with antiferromagnetic (AF) quantum critical point (QCP) are shown, in which $-T^{1/2}$ and $-T^{1/4}$ indicate decrement from some constant values, respectively.

Theories & Materials	$\rho(T)$	$C(T)/T$	$\chi(T)$	$1/T_1 T$	Refs.
CVF	$T^{1.5} \rightarrow T$	$-\log T$	$T^{-\zeta}$	$T^{-\zeta}$	[11–13]
$\text{YbCu}_{5-x}\text{Al}_x$ ($x \simeq 1.5$)	$T^{1.5} \rightarrow T$	$-\log T$	$T^{-0.66}$	*	[1, 2]
YbRh_2Si_2	T	$-\log T$	$T^{-0.6}$	$T^{-0.5}$	[3, 4]
$\beta\text{-YbAlB}_4$	$T^{1.5} \rightarrow T$	$-\log T$	$T^{-0.5}$	*	[7]
$\alpha\text{-YbAl}_{1-x}\text{Fe}_x\text{B}_4$ ($x \simeq 0.014$)	$T^{1.5} \rightarrow T$	$-\log T$	$T^{-0.5}$	*	[8]
$\text{Yb}_{15}\text{Al}_{34}\text{Au}_{51}$	T	$-\log T$	$T^{-0.51}$	$T^{-0.51}$	[9]
$\text{Yb}_{14}\text{Al}_{35}\text{Au}_{51}$ at $P \simeq 1.8$ GPa	T	*	$T^{-0.51}$	*	[19]
AF QCP	$T^{3/2}$	$-T^{1/2}$	$-T^{1/4}$	$T^{-3/4}$	[14–16]

systematic behaviors shown in Table 1 were not observed because such Ce-based compounds are not considered to be just at the valence criticality but in the sharp valence crossover region. CeCu_2Ge_2 is the first example in which anomalous properties characteristic to the sharp valence crossover of Ce ion under pressure around $P = P_v$ was reported [22, 23]. In particular, the superconducting transition temperature exhibits a drastic increase by about triple of that at around the magnetic critical pressure. The T -linear dependence in the resistivity $\rho(T) - \rho_0$, with ρ_0 being the residual resistivity, was also observed at around $P = P_v$, together with a huge enhancement of ρ_0 . After that, similar behaviors have been reported in CeCu_2Si_2 [24], $\text{CeCu}_2\text{Si}_{1.8}\text{Ge}_{0.2}$ [25], and CeRhIn_5 [26, 27], which can be comprehensively understood on the basis of a valence crossover scenario [28, 29]. It was also predicted [30, 31] that the position of the critical point of valence transition is well controlled by the magnetic field, which opens a possibility of realizing the critical point by tuning both pressure and magnetic field simultaneously. Recently, a symptom of such a phenomenon was reported in CeCu_6 [32] which is considered to be located in the crossover region of valence transition [28, 33]. This suggests that the puzzling non-Fermi liquid properties observed in $\text{CeCu}_{6-x}\text{Au}_x$ ($x \simeq 0.1$) [34] should be revisited from the viewpoint of this CVF scenario.

The essence of these intriguing phenomena cannot be captured within the so-called the Doniach paradigm [35] that is essentially based on the Kondo lattice picture in which the valence of Ce and Yb ion is fixed as Ce^{3+} and Yb^{3+} . In other words, we had to develop a conceptually new physics. The purpose of the present paper is to sketch the history and the present status of unconventional phenomena associated with sharp valence crossover or enhanced valence fluctuations in Ce-based heavy fermion metals, and to discuss how these phenomena are ubiquitous than thought previously. The organization of the paper is as follows:

In Sect. 2, we review how the existence of critical point of valence transition in heavy fermion metals was recognized by showing the case of $\text{CeCu}_2(\text{Si,Ge})_2$.

In Sect. 3, we present some fundamental properties of the extended Anderson lattice model (including the Coulomb repulsion between f and conduction electrons) which is the minimal model for describing essential aspects of valence transition and

valence fluctuations observed in Ce- or Yb-based heavy fermion metals.

In Sect. 4, we show that the magnetic field gives appreciable influence on the valence transition of Ce ion discussing the case of CeCu₆.

In Sect. 5, we discuss how the change of the Fermi surface observed in CeRhIn₅ under pressure is understood as a sharp valence crossover phenomenon in a unified fashion without relying on an idea of the destruction of c-f hybridization.

In Sect. 6, summary is given.

2. Sharp crossover in valence of Ce in CeCu₂(Si,Ge)₂

In this section, we discuss a series of experimental evidence suggesting that the valence of Ce exhibits a sharp crossover under pressure in CeCu₂Si₂ [24], resulting in a series of anomalous properties associated with the sharp valence crossover, while such a trend was first reported [22] and discussed theoretically [23] for CeCu₂Ge₂.

A drastic decrement in the A coefficient of the T^2 term in the resistivity, $\rho(T) \simeq \rho_0 + AT^2$, by about two orders of magnitude around the pressure $P = P_v \simeq 4.5$ GPa, as shown in Fig. 1(c), suggests a sharp valence crossover occurs at around $P = P_v$. Note that T_1^{\max} is an increasing function of pressure P and simulates the variation of P . The residual resistivity ρ_0 exhibits a sharp and pronounced peak there, as shown in Fig. 1(b). This implies that the effective mass m^* of the quasiparticles also decreases sharply there, since A is scaled by $(m^*)^2$ [36]. This decrement of m^* implies in turn a sharp change in the valence of Ce ion, deviating from Ce³⁺, considering the fact that the following approximate (but canonical) formula holds in the strongly correlated limit [37, 38]:

$$\frac{m^*}{m_{\text{band}}} = \frac{1 - n_f/2}{1 - n_f}, \quad (1)$$

where m_{band} is the band mass without electron correlations, and n_f is the f-electron number per Ce ion.

Such a sharp crossover in the valence of Ce ion gives rise to a sharp crossover of the so-called Kadowaki-Woods (KW) ratio [36], A/γ^2 , where γ is the Sommerfeld coefficient of the electronic specific heat, from that of a strongly correlated class to a weakly correlated one. Note that γ^{-1} is related to the temperature T_1^{\max} , where the resistivity $\rho(T)$ exhibits maximum, as shown in the inset of Fig. 1(c). This indicates, as discussed in Ref. [39], that the mass enhancement due to the dynamical electron correlation is quickly lost at around $P = P_v$ [39].

This physical picture based on the sharp valence crossover of Ce has been reinforced by ⁶³Cu-NQR measurements in CeCu₂Si₂ at temperature down to $T = 3.1$ K and under pressures up to $P = 5.5$ GPa covering $P_v \simeq 4.5$ GPa [40–42]. Indeed, the NQR frequency ${}^{63}\nu_Q$ rather sharply deviates at above 4 GPa from the linear P -dependence in the low pressure range ($P \leq 3.5$ GPa). The P -dependence of the deviation from the linear dependence in ${}^{63}\nu_Q$ is shown in Fig. 2b). This deviation was estimated to correspond to the change of the valence $\Delta n_f = 0.04$ by the first principles calculations [42]. This degree of change is consistent with the decrease of mass enhancement by ~ 3.9 (~ 15.3 in the A coefficient of the resistivity, as shown in Fig. 1(c)), if the change in n_f would be from $n_f = 0.99$ to $n_f = 0.95$.

In Ref. [42], the change of valence in Ce was estimated from that in NQR frequency ν_Q as follows. On the basis of the LDA calculations, the pressure (P) de-

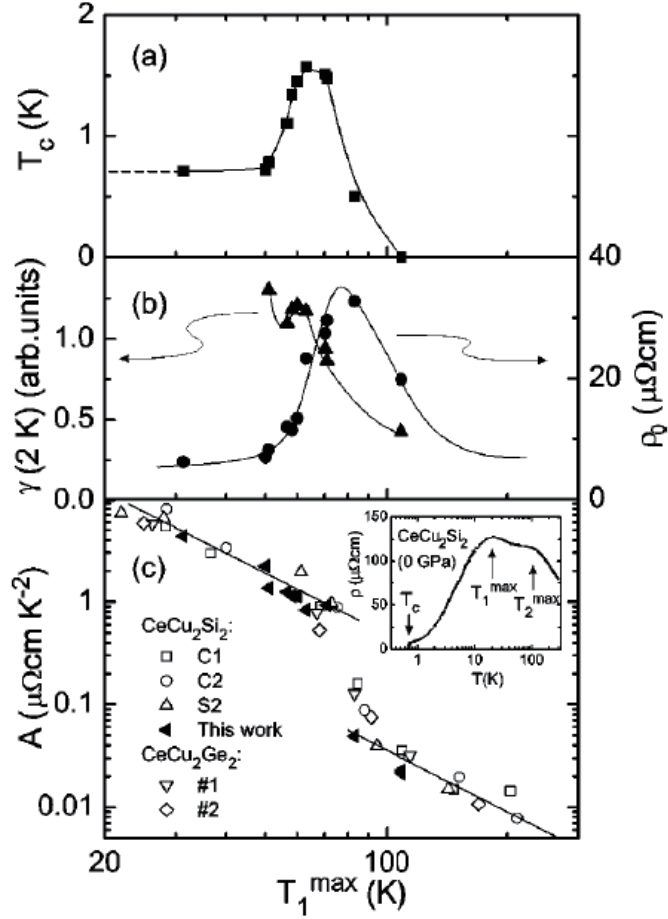


Figure 1. Horizontal axis T_1^{\max} is the characteristic temperature at which the resistivity takes maximum, as shown in inset, and simulates the change in pressure P which increases toward the right-hand side of the scale: (a) the bulk superconducting transition temperature, (b) the residual resistivity and γ coefficient of the electronic specific heat, and (c) the coefficient A of the T^2 -law of the resistivity. The straight lines indicate that the expected $A \propto (T_1^{\max})^{-2}$ scaling is followed. The maximum of T_c coincides with the start of the region where the scaling relation is broken, while the maximum in residual resistivity is situated in the middle of the collapse in A . [24]

pendence of ν_Q for “LaCu₂Si₂” and “CeCu₂Si₂” was estimated with the use of the observed P dependence of the lattice parameter, where f electrons are assumed to be completely localized in the case of “LaCu₂Si₂”, i.e., essentially in $(4f)^0$ configuration, and itinerant but not strongly correlated in the case of “CeCu₂Si₂”. Both show a linear P dependence with similar slopes: $d\nu_Q/dP \simeq 0.103\text{MHz}$ for “LaCu₂Si₂” and $d\nu_Q/dP \simeq 0.089\text{MHz}$ for “CeCu₂Si₂”. However, observed NQR frequency ν_Q of a real CeCu₂Si₂ is located in between because $4f$ electrons in CeCu₂Si₂ are not fully itinerant but have a localized character reflecting strong correlations among $4f$ electrons. Indeed, $\nu_Q(P = 0) \simeq 3.73\text{MHz}$ for “LaCu₂Si₂” and $\nu_Q(P = 0) \simeq 3.02\text{MHz}$ for “CeCu₂Si₂”, while the observed one for the real CeCu₂Si₂ is $\nu_Q(P = 0) \simeq 3.43\text{MHz}$. The deviation in $\nu_Q(P)$ from a P linear dependence shown in Fig. 2(b) reflects a change of electronic contribution to ν_Q , while the linear P dependence reflects the lattice contribution. The amount of deviation $\Delta\nu_Q$ from $P = 3.9$ to $P = 4.5$ is about $\Delta\nu_Q \simeq -0.03\text{MHz}$, which is 3.9% of the differ-

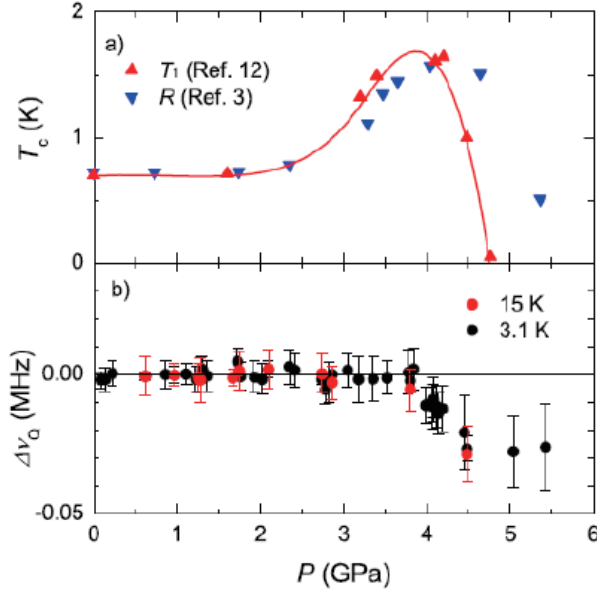


Figure 2. (Color online) Pressure dependence of the superconducting transition temperature T_c and deviation from the linear P dependence of background in the NQR frequency $^{63}\nu_Q$ in CeCu_2Si_2 . [42]

ence $[\nu_Q(\text{"CeCu}_2\text{Si}_2\text{"}) - \nu_Q(\text{"LaCu}_2\text{Si}_2\text{"})] \simeq -0.77\text{MHz}$ at around $P = 3.9\text{-}4.5$ GPa. The negative value of $\Delta\nu_Q$ implies an increase in the itinerant character of 4f electrons, and the ratio of 4f electrons of acquiring itinerant character is estimated as $0.03/0.77 \simeq 0.04$ of the localized component, suggesting $\Delta n_f \simeq 0.04$.

The huge peak of ρ_0 at $P \sim P_V$, as shown in Fig. 1(b), can be explained by the effect that the disturbance in the ratio of numbers of f and conduction electrons around impurity extends to the correlation length ξ_v which grows appreciably toward $P = P_V$ giving rise to strong scattering of quasiparticles. The microscopic justification has been discussed in Ref. [43]. This is in contrast to the effect of AF critical fluctuations on ρ_0 which is rather moderate, as discussed in Ref. [44]. Thus, the critical pressure P_V can be clearly manifested by the maximum of ρ_0 .

Subtle but systematic tendencies shown in Fig. 1 near $P = P_V$ are that the peak of the T_c and the Sommerfeld coefficient $\gamma(T = 2\text{ K})$ appears at slightly lower pressure than P_V . These behaviors can be understood on the basis of explicit theoretical calculations in which almost local valence fluctuations of Ce are shown to develop around the pressure where the sharp valence crossover occurs [24, 28, 45], as supported by the density-matrix-renormalization-group (DMRG) calculation [46].

Another salient property associated with the sharp crossover of the valence is that the temperatures T_i^{max} ($i = 1, 2$), corresponding to two maxima in the resistivity $\rho(T)$, merge at $P \simeq P_V$ as shown in Fig. 3 [24]. Although the existence of the two peaks in $\rho(T)$ and the mergence of them under pressure can be shown theoretically as an effect of smearing crystalline-electric-field (CEF) splitting by the increase of the c-f hybridization under pressure in general [47], it is non-trivial that the mergence occurs at around $P = P_V$. This behavior was also observed in CeCu_2Ge_2 [22], CeAu_2Si_2 [48], and CeAl_2 [49], suggesting a generic property associated with the sharp valence crossover of Ce ion as argued below [24].

A fundamental wisdom is that the so-called Kondo temperature T_K , related to T_i^{max} ($i = 1, 2$), depends crucially on the degeneracy $(2\ell + 1)$ of local f-state: $T_K \sim$

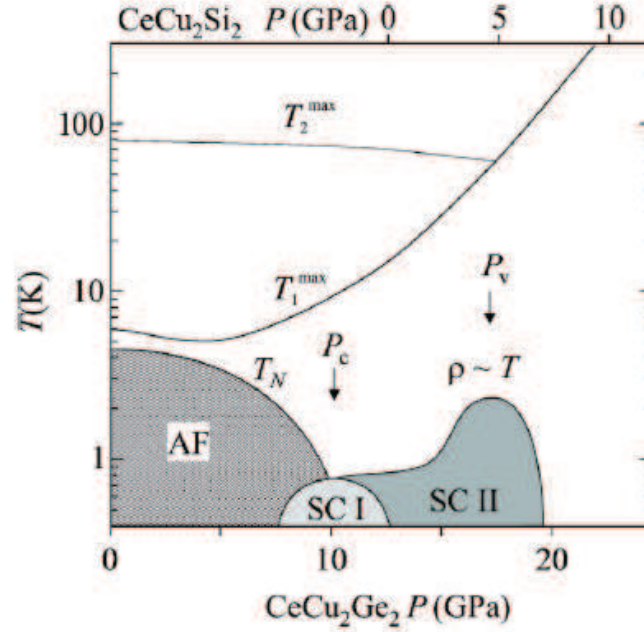


Figure 3. Schematic P - T phase diagram for $\text{CeCu}_2(\text{Si/Ge})_2$ showing the two critical pressures P_c and P_v [24]. At P_c , where the antiferromagnetic ordering temperature $T_N \rightarrow 0$, superconductivity in region SC I is mediated by antiferromagnetic spin fluctuations; around P_v , in the region SC II, valence fluctuations provide the pairing mechanism and the resistivity is linear in temperature. The characteristic temperatures T_1^{\max} and T_2^{\max} merge at a pressure $P \simeq P_v$.

$D \exp[-1/(2\ell + 1)N_F|J|]$, where D is half the bandwidth of conduction electrons, N_F the density of states of conduction electrons at the Fermi level, and J the c-f exchange coupling constant [50]. Furthermore, even though the sixfold degeneracy of local 4f-state is lifted by the CEF effect, leaving the Kramers doublet ground state with the excited CEF levels with excitation energy Δ_{CEF} , the Kondo temperature T_K is still enhanced considerably by the effect of excited CEF levels [51].

It is also crucial to take into account the fact that the practical degeneracy of CEF levels, relevant to the Kondo effect, is affected by the broadening ΔE of the lowest CEF level. If $\Delta E \ll \Delta_{\text{CEF}}$, the degeneracy relevant to T_K is twofold. On the other hand, if $\Delta E > \Delta_{\text{CEF}}$, it increases to fourfold or sixfold. The level broadening is given by $\Delta E \simeq z\pi N_F|V|^2$ where $|V|$ is the strength of c-f hybridization, and z is the renormalization factor which gives the inverse of mass enhancement in the case of lattice systems. Then, it is crucial that ΔE is very sensitive to the valence of Ce ion because z^{-1} is essentially given by eq. (1). In particular, the factor z increases from the tiny value in the Kondo regime, $z \sim (1 - n_f) \ll 1$, and approaches to 1 in the so-called valence fluctuation regime.

Since the factor $\pi N_F|V|^2 \gg \Delta_{\text{CEF}}$ in general for Ce-based heavy fermion metals, the ratio $\Delta E/\Delta_{\text{CEF}}$, which is much smaller than 1 in the Kondo regime, greatly exceeds 1 across the valence transformation around $P \sim P_v$, leading to the increase of the practical degeneracy of f-state, *irrespective* of a sharpness of the valence transformation. Therefore, T_1^{\max} should merge T_2^{\max} , which corresponds to fourfold or sixfold degeneracy of 4 f-state due to the effect of broadening of the CEF ground level. This explains why T_1^{\max} increases and approaches T_2^{\max} at around $P = P_v$.

On the other hand, there have been trials of explaining this mergence of T_i^{\max} ($i = 1, 2$) at around $P = P_v$ as a phenomenon caused by a meta-orbital transition among CEF levels [52] or an interchange of CEF level scheme itself [53]. The latter theoretical prediction contradicts with experimental measurements both of the inelastic neutron scattering [54] and the non-resonant X-ray scattering (NRXS) [55, 56] which shows that the ground state of the CEF levels in CeCu_2Si_2 is $\Gamma_7^1 \simeq -0.88|\pm 5/2\rangle + 0.47|\mp 3/2\rangle$. The former prediction [52] does not immediately contradict with the result of NRXS measurement [56], while it is not so evident whether the condition for the meta-orbital transition to occur is satisfied in the CEF states of CeCu_2Si_2 . Reference [52] assumes much larger c-f hybridization at the first-excited CEF level than that at the ground CEF level. However, the CEF excited state with the c-f hybridization, larger than that of the ground CEF state, seems to correspond to the highest CEF level, $\Gamma_7^2 \simeq 0.47|\pm 5/2\rangle + 0.88|\mp 3/2\rangle$, with excitation energy about 360 K [54].

3. Model for describing valence transition and fluctuations

A canonical model for describing the valence transition due to electronic origin is an extended periodic Anderson model (EPAM) that takes into account the Coulomb repulsion U_{fc} between f and conduction electrons. Explicit form of the EPAM is given as follows:

$$H_{\text{EPAM}} = \sum_{\mathbf{k}\sigma} (\epsilon_{\mathbf{k}} - \mu) c_{\mathbf{k}\sigma}^\dagger c_{\mathbf{k}\sigma} + \varepsilon_f \sum_{\mathbf{k}\sigma} f_{\mathbf{k}\sigma}^\dagger f_{\mathbf{k}\sigma} + U_{\text{ff}} \sum_i n_{i\uparrow}^f n_{i\downarrow}^f + V \sum_{\mathbf{k}\sigma} (c_{\mathbf{k}\sigma}^\dagger f_{\mathbf{k}\sigma} + \text{h.c.}) + U_{\text{fc}} \sum_{i\sigma\sigma'} n_{i\sigma}^f n_{i\sigma'}^c, \quad (2)$$

where U_{fc} is the f-c Coulomb repulsion, which turns out a main origin of valence transition or fluctuations. The label σ in Eq. (2) stands the degrees of freedoms of the Kramers doublet state of the ground CEF level. This model has been discussed in a variety of context [57–62].

The model without hybridization V is called the Falicov-Kimball model (FKM) which has been a canonical model for discussing the valence state of rare earth ions [63, 64]. The condition for the valence transition in the FKM is simply given by

$$\varepsilon_f + n_c U_{\text{fc}} = \mu, \quad (3)$$

where μ is the chemical potential or the Fermi level in the Kondo limit where f electrons are essentially singly occupied, and n_c is the number of conduction electrons at f-site. This relation expresses the competition between the energy level of f-electron modified by the mean field arising from U_{fc} , the f-c Coulomb repulsion, and the Fermi energy of conduction electrons.

Although the existence of the hybridization V makes it difficult to solve the problem, the condition [Eq. (3)] remains to be valid in the mean-field level of approximation. Figure 4 shows the ground state phase diagrams of the EPAM in the ε_f - U_{fc} plane that are obtained by the mean-field approximation using the slave boson technique by taking into account the strong correlation effect ($U_{\text{ff}} = \infty$) [45], and by the DMRG method for the one-dimensional version of the Hamiltonian Eq. (2) with the tight-binding dispersion for the conduction electrons, i.e., $\epsilon_k = -2t \cos ka$ with

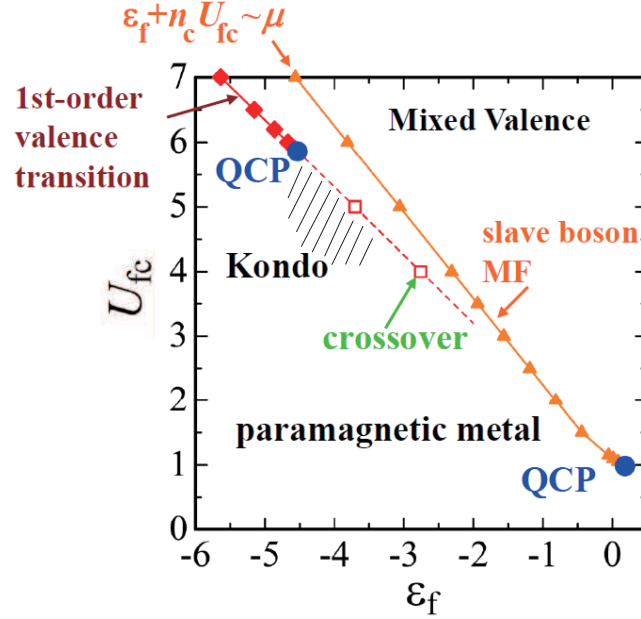


Figure 4. Phase diagram at $T = 0$ of the system described by the Hamiltonian [Eq. (2)] in the ε_f - U_{fc} plane. Triangles are the results by the slave-boson mean-field approximation [45], and diamonds and squares are those by DMRG calculations for one dimensional version of the Hamiltonian [Eq. (2)] in which $\varepsilon_k = -2t \cos ka$ with a being the lattice constant [46]. Solid lines represent the first order valence transition, and dashed line represents the valence crossover from the Kondo to mixed valence regime. Closed circles are critical end point of the first order valence transition, i.e., quantum critical point (QCP) of valence transition. In the shaded region, superconducting correlation with spin-singlet and inter-site pairing dominates over both the SDW and CDW correlations in one dimensional model, suggesting that the d-wave superconductivity is stabilized in this region. Parameters are $V/t = 0.1$, $U_{ff}/t = 100$, and the total electron filling, \bar{n} , is fixed as $\bar{n} = 7/8$, the same as used in Ref. [45]. Unit of U_{fc} and ε_f is also t .

a being the lattice constant [46]. The electron filling $\bar{n} \equiv (n_c + n_f)/2$ is fixed as $\bar{n} = 7/8$ in both calculations. A bunch of calculations on the Gutzwiller variational ansatz have also been performed [65–69]. The first order valence transition (FOVT) line is given essentially by the condition (3) in the mean-field approximation. The quantum critical end point (QCEP), i.e., the quantum critical point (QCP) of the FOVT shown by closed circles, shifts from the position given by the mean-field approximation to that given by asymptotically *exact* DMRG calculation owing to the strong quantum fluctuation effect. In this approach based on EPAM [Eq. (2)], a series of electronic properties associated with the critical valence fluctuations can be *directly* calculated within a required accuracy as summarized in Table 1.

Although the DMRG calculation in one dimension is asymptotically exact, it cannot give a definite conclusion about ordered states. Nevertheless, we can obtain a useful information on the ordered state in higher dimensions by analyzing the dominant long-range correlation function. As shown in Fig. 4, the superconducting tendency with spin-singlet and inter-site pairing dominates over both the SDW and CDW tendencies in the Kondo regime, shaded region, near the crossover line. This suggests that the d-wave superconductivity is stabilized in the Kondo regime near the crossover line, which is consistent with the result obtained by the theory on the basis of slave-boson mean-field solutions supplemented by Gaussian fluctuations around them in the case of three dimensional free dispersion for the conduction

electrons, i.e., $\epsilon_k = k^2/2m$, and with the same electron filling $\bar{n} = 7/8$ [45].

4. Effect of magnetic field on valence transition and crossover: Case of CeCu₆

In this section, the effect of the magnetic field on the critical valence transition or sharp crossover of valence in Ce-based heavy fermion metals is discussed. Since the valence transition or crossover is a phenomenon associated with a charge transfer process or sometimes it is referred to charge fluctuations phenomenon, it appears not to be affected considerably by the magnetic field. However, this is not the case. Indeed, the valence-transition temperature $T_v \simeq 46$ K of α - γ transition at ambient pressure in Ce_{0.8}La_{0.1}Th_{0.1} (without magnetic field) is suppressed to $T_v = 0$ K by the magnetic field of about 50 T [70]. This fact suggests that the position of the QCEP of the valence transition is also greatly influenced by the magnetic field, or the QCEP is easily induced by the magnetic field if the system is located near the QCEP. Indeed, this is the case as discussed below.

The effect of the magnetic field h applied along the z -direction is taken into account by introducing the Zeeman term to the EPAM Hamiltonian [Eq. (2)] as

$$H = H_{\text{EPAM}} - h \sum_i (S_{fi}^z + S_{ci}^z), \quad (4)$$

where S_{fi}^z and S_{ci}^z are z -component of spin of f and conduction electrons, respectively, and the dispersion of conduction electrons in H_{EPAM} [Eq. (2)] is set as $\epsilon_k = k^2/2m - D$, which extends from $-D$ to D . Figure 5 shows how the QCEP of valence transition in the ground state moves by applying magnetic field h on the basis of slave boson mean-field approximation which properly takes into account the correlation effect due to the strong on-site Coulomb interaction U_{ff} in Eq. (4) in the ground state [30, 31]. The unit of energy and magnetic field is taken as D , and the electron filling is fixed as $\bar{n} = 7/8$. The physical meaning of this sensitivity of the position of the QCEP is that the f -electron level of down spin, i.e., $S_{fi}^z < 0$, increases toward the Fermi level by the magnetic field, which promotes the valence transition, as discussed in Refs. [28, 30, 31].

This implies that the magnetic field is a good tuning parameter for searching the QCEP of valence transition. In particular, the QCEP can be precisely hit by simultaneously changing the magnetic field h and the pressure P if the system is located near the QCEP in the ϵ_f - U_{fc} plane at the ambient state, as shown in Fig. 6(a). Indeed, since both U_{fc} and ϵ_f increase as P increases in the Ce-based compounds, the point indicating the location of the system shifts toward right and upper direction as shown in Fig. 6(a). Therefore, the locus of the QCEP due to applying h intersects with that due to applying P .

Recently, a symptom of this phenomenon has been observed in CeCu₆ [32]. Figure 6(b) shows the magnetic field dependence of the A coefficient of the T^2 term in the resistivity under a series of pressures P s. At ambient pressure, A is an almost monotonically decreasing function of H . By increasing pressure, it begins to show a clear maximum at H_m where the metamagnetic sharp increase in the magnetization is observed. Note that A is shown in a logarithmic scale. Variations of the A coefficient is rather prominent if it is plotted in a linear scale, as shown in Fig. 6(c) where A is scaled by $A(0)$ at ambient pressure and H is scaled by the metamagnetic field H_m .

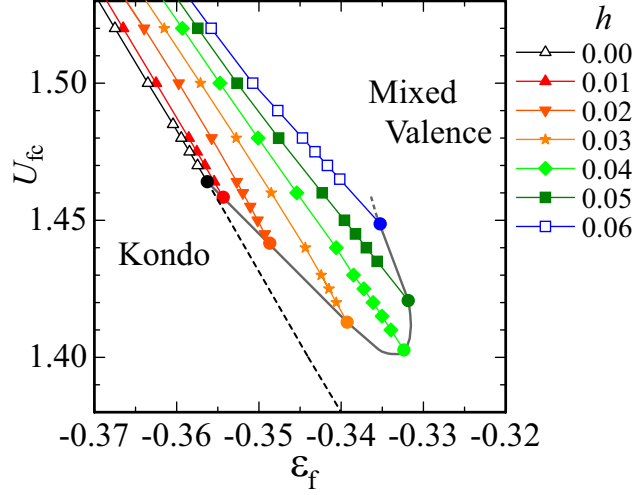


Figure 5. (color online) Ground-state phase diagram in the plane of $U_{fc} - \epsilon_f$ for $D = 1$, $V = 0.5$ at the electron filling $\bar{n} = 7/8$. The FOVT line with a QCP for $h = 0.00$ (open triangle), $h = 0.01$ (filled triangle), $h = 0.02$ (filled inverse triangle), $h = 0.03$ (filled star), $h = 0.04$ (filled diamond), $h = 0.05$ (filled square) and $h = 0.06$ (open square). The curve connects the QCP under h , which is a guide for the eyes. The dashed line represents the valence-crossover points at which $\chi_v \equiv -(\partial n_f / \partial \epsilon_f)$ has a maximum as a function of ϵ_f for each U_{fc} at $h = 0.00$ [30, 31].

The peak structure becomes sharper and sharper as P increases, which strongly suggests that A diverges at the QCEP because the T dependence of the resistivity should exhibit the T -linear dependence there. Experiments at higher pressure and magnetic field are highly desired.

Indeed, it has already been reported that CeCu_6 is located near the QCEP of valence transition and a sharp valence crossover occurs at $P \simeq 5$ GPa, although the decrement in the A coefficient against the pressure is slightly moderate compared to that in CeCu_2Si_2 and CeCu_2Ge_2 [28, 33]. A characteristic temperature T_F^* (or the effective Fermi energy ϵ_F^*) of CeCu_6 is very low of the order of 10 K reflecting the heaviness of its effective mass. This suggests that the QCEP is recovered by the magnetic field of the order of T_F^* , i.e., $H \gtrsim 10$ T and under a certain pressure $P_c > 2$ GPa, which is in consistent with the experiment reported in Ref. [32]. This physical picture is also consistent with the disappearance of magnetic correlations in the region $H \gtrsim 2.5$ T, which was observed by the inelastic neutron scattering experiment [71].

The heavy fermion compound CeRu_2Si_2 , exhibiting metamagnetic behavior, is also expected to exhibit a valence transition at $P \sim 4$ GPa, offering us another candidate for investigating the effect of magnetic field on valence transition [72].

5. Signature of sharp valence crossover in CeRhIn_5 under pressure

CeRhIn_5 is one of prototypical heavy fermion systems well studied experimentally. Its phase diagram is shown in Fig. 7: (a) in the P - H plane at $T = 0$ K, and (b) in the P - T plane at $H = 0$ [26]. Other than the coexistence of superconductivity and antiferromagnetic or the proximity of them across the discontinuous phase boundary under pressure [26, 27], the de Haas-van Alphen (dHvA) measurement

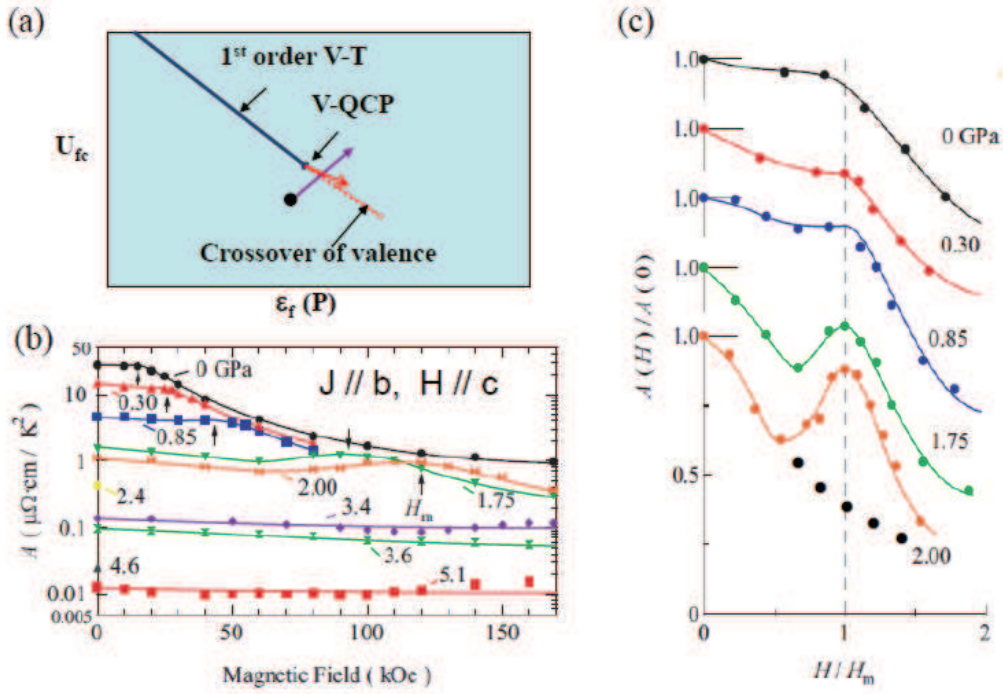


Figure 6. (color online) (a) Schematic view how the critical end point is tuned by pressure P and magnetic field H . Large and small closed circles represent the position of the system and the QCEP, respectively. A line with arrow from the system point indicates the locus of the system point as P increases, and a red line with arrow from the QCEP indicates the locus of QCEP as h increases. (b) The magnetic field (H) dependence of the A coefficient of the T^2 term in the resistivity $\rho(T)$ in the logarithmic scale under a series of pressures P s [32]. Vertical arrows indicate the metamagnetic field H_m for each pressure. (c) Scaled relation between the A coefficient and the magnetic field H for a series of pressures P s [32]. A series of closed circles at $P = 2.00$ GPa is a guide to the eye showing a possible background variation of A not related to the valence crossover.

performed along the line $H \simeq 15$ Tesla (indicated by an arrow) in Fig. 7(a) revealed the following remarkable facts [74]:

- The Fermi surfaces change at $P = P_c$ from those expected for localized f electrons (giving no contribution to the Fermi volume as in LaRhIn₅) to those for itinerant f electrons contributing to the Fermi volume.
- The cyclotron mass exhibits a sharp peak at around $P = P_c$ even though the magnetic transition is the first order and is not associated with AF critical fluctuations.

These aspects are explained naturally as a phenomenon associated with the valence crossover of Ce ion on the basis of the EPAM Hamiltonian defined by Eq. (2) [75, 76]. Characteristic of our theory is that the first order magnetic transition is not accompanied by the localization of f electrons in the magnetic phase but remains itinerant with mass enhancement of quasiparticles, which is consistent with experiments [74]. This is in marked contrast to the local criticality theory on the so-called Kondo breakdown idea [77–79] in which the c-f hybridization in the AF phase is completely vanishing.

The relation between AF order and valence transition or sharp crossover can be

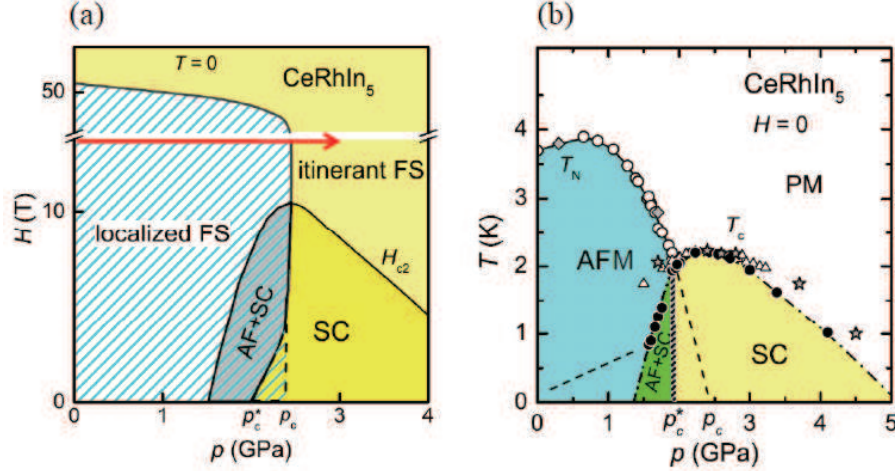


Figure 7. (Color online) (a) Phase diagram of CeRhIn₅ at $T \rightarrow 0$ K in P - H plane. [26] (b) Phase diagram of CeRhIn₅ without magnetic field ($H = 0$ Tesla) in P - T plane [26]. The dashed line indicates the superconducting transition temperature reported in Ref. [73].

understood on the EPAM [Eq. (2)] by treating it in the mean-field approximations both for the AF order and the slave boson which is introduced to take into account the strong local correlation effect between on-site f electrons [75, 76]. In order to simulate the above two facts observed in dHvA experiment, the dispersion of conduction electrons is set as

$$\epsilon_k = -2t(\cos k_x a + \cos k_y a), \quad (5)$$

which simulates the two dimensional β_2 -branch observed by the dHvA measurements in Ref. [74].

Figure 8(a) shows the phase diagram in the ground state of EPAM [Eq. (2)], with the conduction electron dispersion given by Eq. (5), in the ϵ_f - U_{fc} plane for the parameter set $t = 1$, $V = 0.2$, $U = \infty$ and the electron filling $\bar{n} = 0.9$ [75]. A remarkable aspect is that the line of first-order valence-transition (shown by solid line with triangles) and that of valence crossover (shown by dashed line with open circles) almost coincides with the boundary between AF and paramagnetic phase (shown by solid line with squares). A solid circle represents the QCEP of valence transition. Figure 8(b) shows the valence susceptibility $\chi_v \equiv -(\partial n_f / \partial \epsilon_f)$ which exhibits clear maxima on the line of valence crossover. Namely, the AF order is cut by the valence transition or valence crossover [80]. Figure 8(c) shows the ϵ_f dependence of the AF order parameter m_s exhibiting the first order transition at $\epsilon_f = 0.283$.

Figure 9(a) shows the change of the Fermi wave number k_F along the line of $k_x = k_y$ for the parameter set $t = 1$, $V = 0.2$, $U = \infty$, $U_{fc} = 0.5$, and the electron filling $\bar{n} \equiv (n_c + n_f)/2 = 0.9$ under the magnetic field $h = 0.005$ with the Hamiltonian [Eq. (4)] [75]. This shows that, associated with the onset of AF state by the first order transition, the Fermi surface changes discontinuously from the smaller size to the larger one as if the f -electrons were localized in the AF state or the transition to AF state were accompanied by the localization of f electrons. This is because the k_F in the AF state almost coincides with k_F^c of the conduction electrons with the filling $\bar{n}_c \equiv (n_c/2) = 0.4$ since $\bar{n}_c = n - (n_f/2) = 0.9 - (n_f/2)$ is reduced to $\bar{n}_c = 0.4$

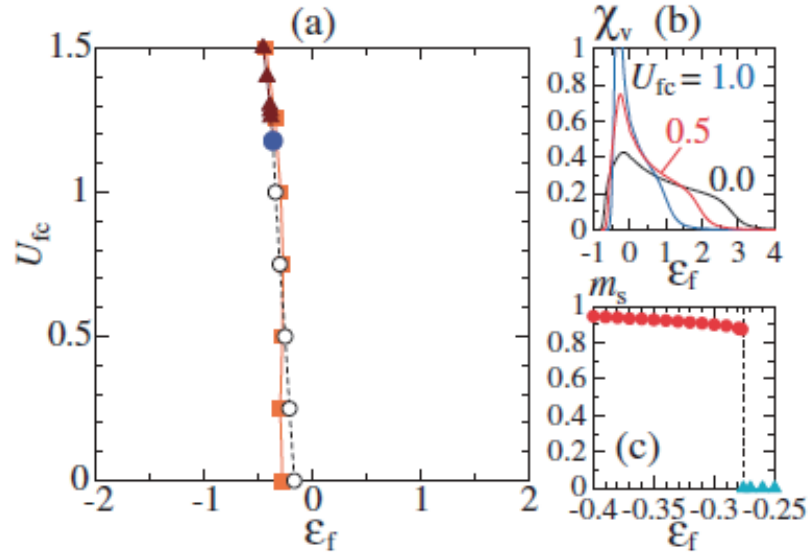


Figure 8. (color) (a) Ground-state phase diagram in the ε_f - U_{fc} plane for paramagnetic and AF states. The first-order valence-transition line (solid line with triangles) terminates at the QCEP of valence transition (filled circle). Valence crossover occurs at the dashed line with open circles, where χ_v has a maximum, as shown in (b). The solid line with squares represents the boundary between the AF state and the paramagnetic state. (c) AF order parameter m_s vs ε_f for $U_{fc} = 0.5$. All results in (a)-(c) are calculated for $t = 1$, $V = 0.2$, $U = \infty$, and the electron filling $\bar{n} \equiv (n_c + n_f)/2 = 0.9$ [75].

if the number of f electron per Ce is $n_f = 1.0$ corresponding to the “localization” of f-electrons at each Ce site. However, it is not the case. Indeed, the quasiparticles consist both of f- and conduction electrons there, and their effective mass is still enhanced in consistent with specific heat measurement in CeRhIn₅ [81, 82], showing that the Sommerfeld constant in the AF state $\gamma = 50$ mJ/mol·K² is about 10 times larger than $\gamma = 5.7$ mJ/mol·K² in LaRhIn₅. The origin of small Fermi surface is the effect of the band folding associated with the onset of the AF ordering [75], but not that of the localization of f electrons [77–79].

The enhancement in observed cyclotron mass, near the phase boundary of AF and paramagnetic states, is reproduced theoretically, as shown in Fig. 9(b). The origin of this enhancement is the band effect of folding or unfolding of the Fermi surface associated with the AF transition, which is in consistent with the above picture of the change of the Fermi surface at the transition [75].

To summarize the above discussions, the characteristic aspects a) and b) of CeRhIn₅ obtained by the dHvA experiments [74], listed in P. 11, can be understood in a unified way as a phenomenon associated with the valence crossover of Ce ion under the pressure and the magnetic field.

Other circumstantial evidence for the sharp valence crossover to be realized in CeRhIn₅ at $P = P_c$ is summarized as follows:

- 1) The resistivity at $T = 2.25$ K just above T_c exhibits huge peak at around $P = P_c$ [26, 83], which is a reminiscent of the case of CeCu₂(Si,Ge)₂. This indicates that the valence fluctuations are enhanced around $P = P_c$, as discussed in Ref. [43].

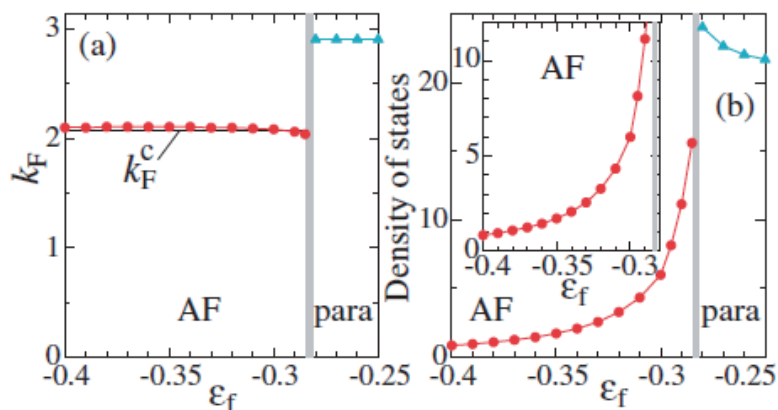


Figure 9. (color) (a) Fermi wave number k_F vs ϵ_f in the AF state (circles) and the paramagnetic state (triangles) for $t = 1$, $V = 0.2$, $U = \infty$, $U_{fc} = 0.5$, and the electron filling $\bar{n} \equiv (n_c + n_f)/2 = 0.9$ under the magnetic field $h = 0.005$. The solid line represents k_F for the conduction band ϵ_k at $\bar{n}_c = 0.4$. (b) Density of states at the Fermi level $D(\mu)$ vs ϵ_f for the same parameters as (a). The inset is enlargement of the AF phase [75].

- 2) The exponent of α , in $[\rho(T) - \rho_0] \propto T^\alpha$, approaches 1 near $P = P_c$, as demonstrated in Ref. [27]. This gives the signature of existence of critical valence fluctuations [24].
- 3) The so-called Kadowaki-Wood scaling, $\sqrt{A}/m^* = \text{const.}$, holds at $P \lesssim P_c$, while both A and m^* grow steeply as P approach P_c from the lower pressure side. This implies that the divergent behaviors in A and m^* are not due to the AF critical fluctuations which would make $A/(m^*)^2$ diverge there.

Concluding this section, we here discuss a symptom suggesting the existence of the QCEP of the valence transition on the phase boundary between AF and paramagnetic state (at $P \simeq P_c$) at higher magnetic field outside the region explored experimentally so far. A crucial point is that the pressure dependence of the SC transition temperature T_c and the upper critical field H_{c2} are quite different (see Fig. 7). Namely, the former is almost flat at $P \gtrsim P_c$ [Fig. 7(a)] while the latter prominently increases as the pressure approaches P_c [Fig. 7(b)]. This suggests that the SC pairing interaction is promoted by the magnetic field H . One of such possibilities is that the QCEP of valence transition is located at the magnetic field $H = H^*$ (> 10 Tesla) on the phase boundary at $P = P_c$ between the AF and the paramagnetic state in the phase diagram Fig. 7(a). This is reasonable, considering the fact that its phase boundary coincides with the valence crossover lines as shown in Fig. 8 [75], and the SC state is stabilized in the region where a sharp crossover of valence occurs [24, 28, 45, 46].

It is also interesting to note that a similar trend can be seen in CeIrSi_3 [84] and CeRhSi_3 [85]. Indeed, Fig. 10(a) shows the $P - T$ phase diagram of CeIrSi_3 [84], in which the pressure \bar{P}_c , where the smooth extrapolation of the Néel temperature T_N in the SC phase vanishes, and the pressure P_c^* , where the SC transition temperature T_{sc} takes a broad maximum, is markedly different. Furthermore, the uppercritical field H_{c2} exhibits a sharp and huge enhancement around $P = P_c^*$, as shown in Fig. 10(b). This implies that the pairing interaction is increased sharply as the magnetic

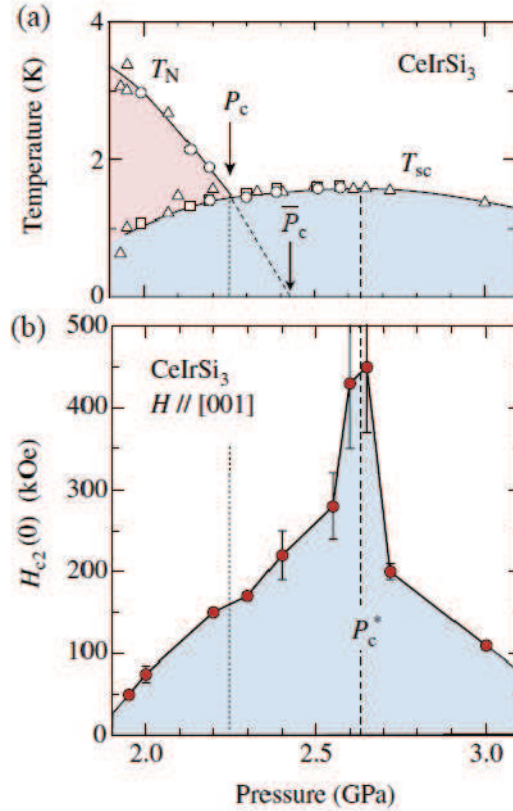


Figure 10. (Color online) (a) $P - T$ phase diagram of CeIrSi₃ without magnetic field, i.e., $H = 0$. P_c is defined as the pressure where the Néel temperature T_N coincides with the superconducting transition temperature T_{sc} [84], and P_c^* is a hypothetical critical pressure where the T_N extrapolated into the SC phase vanishes. (b) Upper-critical field $H_{c2}(T \rightarrow 0)$ as a function of P . $H_{c2}(T \rightarrow 0)$ takes sharply enhanced maximum at P_c^* , where the T_{sc} takes a broad maximum at $H = 0$ [84].

field H is increased, suggesting that the QCEP of valence transition is induced by the magnetic field at around $P = P_c^*$ as in the case of CeRhIn₅ at $P = P_c$ shown in Fig. 7, although the definition of $P = P_c$ and $P = P_c^*$ are different in these two references [84] and [26]. We also note that a similar enhancement of H_{c2} was observed in UGe₂ at $P \gtrsim P_x$ [86], which was explained nicely by the effect that the pairing interaction is enhanced by the effect of field induced magnetic transition between two types of ferromagnetic states in UGe₂ [87].

6. Summary

We have presented a story how the idea of the critical valence transition or sharp valence crossover of heavy fermion metals has been developed, and how these phenomena are ubiquitous than first thought in the beginning of the present century. Although we have discussed relatively well established cases, there would be other potential systems which have not been well recognized so far.

Acknowledgements

We acknowledge J. Flouquet, A. T. Holmes, D. Jaccard, H. Maebashi, O. Narikiyo, Y. Onishi, and A. Tsuruta for long collaborations on physics of critical valence fluctuations on which a considerable part of the present article is based. Discussions and conversations with K. Deguchi, K. Fujiwara, H. Kobayashi, T. C. Kobayashi, K. Kuga, Y. Matsumoto, S. Nakatsuji, and N. K. Sato on experimental data are also acknowledged. This work is supported by the Grant-in-Aid for Scientific Research (No. 24540378, No. 25400369, No. 15K05177, and No. 16H01077) from the Japan Society for the Promotion of Science. One of us (S.W.) was supported by JASRI (Proposal No. 0046 in 2012B, 2013A, 2013B, 2014A, 2014B, and 2015A).

References

- [1] E. Bauer, E.-W. Scheidt, E. Bauer, and G. R. Stewart, *Onset of magnetic order in YbCu_{5-x}Al_x*, Phys. Rev. B **56** (1997) p.711.
- [2] C. Seuring, K. Heuser, E.-W. Scheidt, T. Schreiner, E. Bauer, G. R. Stewart, *Evidence of field-induced non-Fermi-liquid behavior in YbCu_{5-x}Al_x compounds*, Physica B **281** (2000) p.374.
- [3] O. Trovarelli, C. Geibel, S. Mederle, C. Langhammer, F. M. Grosche, P. Gegenwart, M. Lang, G. Sparn, and F. Steglich, *YbRh₂Si₂: Pronounced non-Fermi-liquid effects above a low-lying magnetic phase transition*, Phys. Rev. Lett. **85** (2000) p. 626.
- [4] K. Ishida, K. Okamoto, Y. Kawasaki, Y. Kitaoka, O. Trovarelli, C. Geibel, and F. Steglich, *YbRh₂Si₂: Spin fluctuations in the vicinity of a quantum critical point at low magnetic field*, Phys. Rev. Lett. **89** (2002) p.107202.
- [5] A. Yamamoto, S. Wada, and J. L. Sarrao, *Quantum criticality of the heavy-fermion compound YbAuCu₄*, J. Phys. Soc. Jpn. **76** (2007) p.063709.
- [6] S. Wada, A. Yamamoto, K. Ishida, and J. L. Sarrao, *Competition between valence and spin fluctuations in the vicinity of the quantum critical point of the heavy fermion compound YbAuCu₄*, J. Phys.: Condens. Matter **20** (2008) p.175201.
- [7] S. Nakatsuji, K. Kuga, Y. Machida, T. Tayama, T. Sakakibara, Y. Karaki, H. Ishimoto, S. Yonezawa, Y. Maeno, E. Pearson, G. G. Lonzarich, L. Balicas, H. Lee, and Z. Fisk., *Superconductivity and quantum criticality in the heavy-fermion system β -YbAlB₄*, Nat. Phys. **4** (2008) p.603.
- [8] K. Kuga and S. Nakatsuji, private communication.
- [9] K. Deguchi, S. Matsukawa, N. K. Sato, T. Hattori, K. Ishida, H. Takakura, and T. Ishimasa, *Quantum critical state in a magnetic quasicrystal*, Nat. Mater. **11** (2012) p.1013; private communication.
- [10] S. Matsukawa, K. Deguchi, K. Imura, T. Ishimasa, and N. K. Sato, *Pressure-driven quantum criticality and T/H scaling in the icosahedral Au-A-Yb approximant*, J. Phys. Soc. Jpn. **85** (2016) p.063706.
- [11] S. Watanabe and K. Miyake, *Quantum valence criticality as an origin of unconventional critical phenomena*, Phys. Rev. Lett. **105** (2010) p.186403.
- [12] S. Watanabe and K. Miyake, *Robustness of quantum criticality of valence fluctuations*, J. Phys. Soc. Jpn. **82** (2013) p.083704.
- [13] S. Watanabe and K. Miyake, *New universality class of quantum criticality in Ce- and Yb-based heavy fermions*, J. Phys.: Condens. Matter **24** (2012) p.294208.
- [14] T. Moriya and T. Takimoto, *Anomalous properties around magnetic instability in heavy electron systems*, J. Phys. Soc. Jpn. **64** (1995) p.960.
- [15] M. Hatatani, O. Narikiyo and K. Miyake, *A theory of uniform spin susceptibility around the antiferromagnetic quantum critical point*, J. Phys. Soc. Jpn. **67** (1998) p.4002.
- [16] M. Hatatani, *Nature of critical spin fluctuations around the quantum critical point*, PhD Thesis, 2000, Graduate School of Engineering Science, Osaka University.
- [17] Y. Matsumoto, S. Nakatsuji, K. Kuga, Y. Karaki, N. Horie, Y. Shimura, T. Sakakibara, A. H. Nevidomskyy, and P. Coleman, *Quantum criticality without tuning in the mixed valence compound β -YbAlB₄*, Science **331** (2011) p.316.
- [18] Y. Matsumoto, K. Kuga, Y. Karaki, Y. Shimura, T. Sakakibara, M. Tokunaga, K. Kindo, and S. Nakatsuji, *Field evolution of quantum critical and heavy Fermi-liquid components in the magnetization of the mixed valence compound β -YbAlB₄*, J. Phys. Soc. Jpn. **84** (2015) p.024710.
- [19] K. Deguchi and N. K. Sato, private communication.
- [20] S. Watanabe and K. Miyake, *T/B Scaling in β -YbAlB₄*, J. Phys. Soc. Jpn. **83** (2014) p.103708.
- [21] S. Watanabe and K. Miyake, *Origin of quantum criticality in Yb-Al-Au approximant crystal and quasicrystal*, J. Phys. Soc. Jpn. **85** (2016) p.063703.
- [22] D. Jaccard, H. Wilhelm, K. Alami-Yadri, E. Vargoz, *Magnetism and superconductivity*

- in heavy fermion compounds at high pressure*, Physica B **259-261** (1999) p.1.
- [23] K. Miyake, O. Narikiyo, and Y. Onishi, *Superconductivity of Ce-based heavy fermions under pressure: Valence fluctuation mediated pairing associated with valence instability of Ce*, Physica B **259-261** (1999) p.676.
- [24] A. T. Holmes, D. Jaccard, and K. Miyake, *Signatures of valence fluctuations in CeCu₂Si₂ under high pressure*, Phys. Rev. B **69** (2004) p.024508.
- [25] H. Q. Yuan, F. M. Grosche, M. Deppe, C. Geibel, G. Sparn, and F. Steglich, *Observation of two distinct superconducting phases in CeCu₂Si₂*, Science **302** (2003) p.2104.
- [26] G. Knebel, D. Aoki, J.-P. Brison, and J. Flouquet, *The quantum critical point in CeRhIn₅: A resistivity study*, J. Phys. Soc. Jpn. **77** (2008) p.114704.
- [27] T. Park, V. A. Sidorov, F. Ronning, J.-X. Zhu, Y. Tokiwa, H. Lee, E. D. Bauer, R. Movshovich, J. L. Sarrao, and J. D. Thompson, *Isotropic quantum scattering and unconventional superconductivity*, Nature **456** (2008) p.366.
- [28] K. Miyake, *New trend of superconductivity in strongly correlated electron systems*, J. Phys.: Condens. Matter **19** (2007) p.125201.
- [29] K. Miyake and S. Watanabe, *Unconventional quantum criticality due to critical valence transition*, J. Phys. Soc. Jpn. **83** (2014) p.061006.
- [30] S. Watanabe, A. Tsuruta, K. Miyake, and J. Flouquet, *Magnetic-field control of quantum critical points of valence transition*, Phys. Rev. Lett. **100** (2008) p.236401.
- [31] S. Watanabe, A. Tsuruta, K. Miyake, and J. Flouquet, *Valence fluctuations revealed by magnetic field and pressure scans: Comparison with experiments in YbXCu₄ (X=In, Ag, Cd) and CeYIn₅ (Y=Ir, Rh)*, J. Phys. Soc. Jpn. **78** (2009) p.104706.
- [32] Y. Hirose, J. Sakaguchi, M. Ohya, M. Matsushita, F. Honda, R. Settai, and Y. Ōnuki, *Collapse and enhancement of the heavy fermion state in CeCu₆ under magnetic field and pressure*, J. Phys. Soc. Jpn. **81** (2012) p.SB009.
- [33] S. Raymond and D. Jaccard, *High pressure resistivity of the heavy fermion compound CeCu₆*, J. Low Temp. Phys. **120** (2000) p.107.
- [34] H. v. Löhneysen, A. Rosch, M. Vojta, and P. Wölfle, *Fermi-liquid instabilities at magnetic quantum phase transitions*, Rev. Mod. Phys. **79** (2007) p.1015.
- [35] S. Doniach, *The Kondo lattice and weak antiferromagnetism*, Physica B **91** (1977) p.231.
- [36] K. Kadowaki and S. B. Woods, *Universal relationship of the resistivity and specific heat in heavy-fermion compounds*, Solid State Commun. **58** (1986) p.507.
- [37] T. M. Rice and K. Ueda, *Gutzwiller method for heavy electrons*, Phys. Rev. B **34** (1986) p.6420.
- [38] H. Shiba, *Properties of strongly correlated Fermi liquid in valence fluctuation system -A variational Monte-Carlo study*, J. Phys. Soc. Jpn. **55** (1986) p.2765.
- [39] K. Miyake, T. Matsuura, and C. M. Varma, *Relation between resistivity and effective mass in heavy-fermion and A15 compounds*, Solid State Commun. **71** (1989) p.1149.
- [40] K. Fujiwara, Y. Hata, K. Kobayashi, K. Miyoshi, J. Takeuchi, Y. Shimaoka, H. Kotegawa, T. C. Kobayashi, C. Geibel, and F. Steglich, *High pressure NQR measurement in CeCu₂Si₂ up to sudden disappearance of superconductivity*, J. Phys. Soc. Jpn. **77** (2008) p.123711.
- [41] K. Fujiwara, M. Iwata, Y. Okazaki, Y. Ikeda, S. Araki, T. C. Kobayashi, K. Murata, C. Geibel, and F. Steglich, *Cu-NQR of CeCu₂Si₂ under high pressure*, J. Phys.: Conf. Ser. **391** (2012) p.012012.
- [42] T. C. Kobayashi, K. Fujiwara, K. Takeda, H. Harima, Y. Ikeda, T. Adachi, Y. Ohishi, C. Geibel, and F. Steglich, *Valence crossover of Ce ions in CeCu₂Si₂ under high pressure -Pressure dependence of the unit cell volume and the NQR frequency-*, J. Phys. Soc. Jpn. **82** (2013) p.114701.
- [43] K. Miyake and H. Maebashi, *Huge enhancement of impurity scattering due to critical valence fluctuations in a Ce-based heavy electron system*, J. Phys. Soc. Jpn. **71** (2002) p.1007.
- [44] K. Miyake and O. Narikiyo, *Enhanced impurity scattering due to quantum critical*

- fluctuations: Perturbational approach*, J. Phys. Soc. Jpn. **71** (2002) p.867.
- [45] Y. Onishi and K. Miyake, *Enhanced valence fluctuations caused by f-c Coulomb interaction in Ce-based heavy electrons: Possible origin of pressure-induced enhancement of superconducting transition temperature in CeCu₂Ge₂ and related compounds*, J. Phys. Soc. Jpn. **69** (2000) p.3955.
- [46] S. Watanabe, M. Imada, and K. Miyake, *Superconductivity emerging near quantum critical point of valence transition*, J. Phys. Soc. Jpn. **75** (2006) p.043710.
- [47] Y. Nishida, A. Tsuruta, and K. Miyake, *Crystalline-electric-field effect on the resistivity of Ce-based heavy fermion systems*, J. Phys. Soc. Jpn. **75** (2006) p.064706.
- [48] Z. Ren, G. Girit, G. W. Scheerer, G. Lapertot, and D. Jaccard, *Effect of disorder on the pressure-induced superconducting state of CeAu₂Si₂*, Phys. Rev. B **91** (2015) p.094515.
- [49] B. Barbara, J. Beille, B. Cheaito, J. M. Laurant, M. F. Rossignol, A. Waintal, and S. Zemirli, *On the pressure-temperature phase diagram of the Kondo compound CeAl₂*, J. Phys. (Paris) **48** (1987) p.635.
- [50] A. Ogawa and A. Yoshimori, *Effects of anisotropy energy on the ground state of Ce impurities in metals*, Prog. Theor. Phys. **53** (1975) p.351.
- [51] K. Yamada, K. Yoshida, and K. Hanzawa, *Fermi liquid theory on the basis of periodic Anderson hamiltonian with orbital degeneracy*, Prog. Theor. Phys. **71** (1984) p.450.
- [52] K. Hattori, *Meta-orbital transition in heavy-fermion systems: Analysis by dynamical mean field theory and self-consistent renormalization theory of orbital fluctuations*, J. Phys. Soc. Jpn. **79** (2010) p.114717.
- [53] L. V. Pourovskii, P. Hansmann, M. Ferrero, and A. Georges, *Theoretical prediction and spectroscopic fingerprints of an orbital transition in CeCu₂Si₂*, Phys. Rev. Lett. **112** (2014) p.106407.
- [54] S. Horn, E. Holland-Moritz, M. Loewenhaupt, F. Steglich, H. Scheuer, A. Benoit, and J. Flouquet, *Magnetic neutron scattering and crystal-field states in CeCu₂Si₂*, Phys. Rev. B **23** (1981) p.3171.
- [55] T. Willers, F. Strigari, N. Hiraoka, Y. Q. Cai, M. W. Haverkort, K.-D. Tsuei, Y. F. Liao, S. Seiro, C. Geibel, F. Steglich, L. H. Tjeng, and A. Severing, *Determining the In-Plane Orientation of the Ground-State Orbital of CeCu₂Si₂*, Phys. Rev. Lett. **109** (2012) p.046401.
- [56] J.-P. Rueff, J. M. Ablett, F. Strigari, M. Deppe, M. W. Haverkort, L. H. Tjeng, and A. Severing, *Absence of orbital rotation in superconducting CeCu₂Ge₂*, Phys. Rev. B **91** (2015) p.201108.
- [57] A. C. Hewson and P. S. Riseborough, *An exact limit of a local mixed valence model*, Solid State Commun. **22** (1977) p.379.
- [58] P. Schlottmann, *Simple spinless mixed-valence model. I. Coherent-hybridization states versus virtual-bound states*, Phys. Rev. B **22** (1980) p.613.
- [59] T. A. Costi and A. C. Hewson, *Static and dynamic properties of the Anderson model with conduction electron screening*, Physica C **185-189** (1991) p.2649.
- [60] R. Takayama and O. Sakai, *Excitation spectra of the Anderson model with charge screening through d-f Coulomb interaction*, J. Phys. Soc. Jpn. **66** (1997) p.1512.
- [61] I. E. Perakis and C. M. Varma, *Non-Fermi-liquid states of a magnetic ion in a metal: Particle-hole symmetric case*, Phys. Rev. B **49** (1994) p.9041.
- [62] D. I. Khomskii and A. N. Kocharjan, *Virtual levels, mixed valence phase and electronic phase transitions in rare earth compounds*, Solid State Commun. **18** (1976) p.985.
- [63] L. M. Falicov and J. C. Kimball, *Simple model for semiconductor-metal transitions: SmB₆ and transition-metal oxides*, Phys. Rev. Lett. **22** (1969) p.997.
- [64] C. M. Varma, *Mixed-valence compounds*, Rev. Mod. Phys. **48** (1976) p.219.
- [65] Y. Onishi and K. Miyake, *Sharp valence transition caused by f-c Coulomb interaction in an extended periodic Anderson model*, Physica B **281&282** (2000) p.191.
- [66] Y. Saiga, T. Sugibayashi, and D. S. Hirashima, *Valence instability and the quantum critical point in an extended periodic Anderson model: Analysis based on the dynamical*

- mean field theory*, J. Phys. Soc. Jpn. **77** (2008) p.114710.
- [67] T. Sugibayashi, A. Tsuruta, and K. Miyake, *Valence fluctuations in an extended periodic Anderson model under a magnetic field*, Physica C **470** (2010) p.S550.
- [68] K. Kubo, *Gutzwiller method for an extended periodic Anderson model with the c-f Coulomb interaction*, J. Phys. Soc. Jpn. **80** (2011) p.114711.
- [69] I. Hagymasi, K. Itai, and J. Solyom, *Periodic Anderson model with d-f interaction*, Acta Phys. Pol. A **121** (2012) p.1070.
- [70] F. Drymiotis, J. Singleton, N. Harrison, L. Balicas, A. Bangura, C. H. Mielke, Z. Fisk, A. Migliori, J. L. Smith, and J. C. Lashley, *Suppression of the γ - α structural phase transition in $\text{Ce}_{0.8}\text{La}_{0.1}\text{Th}_{0.1}$ by large magnetic fields*, J. Phys.: Condens. Matter **17** (2005) p.L77.
- [71] J. Rossat-Mignod, L. P. Renault, J. L. Jacoud, C. Vettier, P. Lejay, J. Flouquet, E. Walker, D. Jaccard, and A. Amato, *Inelastic neutron scattering study of cerium heavy fermion compounds*, J. Magn. Magn. Mater. **76-77** (1988) p.376.
- [72] J. Flouquet, Y. Haga, P. Haen, D. Braithwaite, G. Knebel, S. Raymond, and S. Kambe, *Phase diagram of heavy fermion systems*, J. Magn. Magn. Mater. **272-276** (2004) p.27.
- [73] G. F. Chen, K. Matsubayashi, S. Ban, K. Deguchi, and N. K. Sato, *Competitive coexistence of superconductivity with antiferromagnetism in CeRhIn_5* , Phys. Rev. Lett. **97** (2006) p.017005.
- [74] H. Shishido, R. Settai, H. Harima, and Y. Ōnuki, *A drastic change of the Fermi surface at a critical pressure in CeRhIn_5 : dHvA study under pressure*, J. Phys. Soc. Jpn. **74** (2005) p.1103.
- [75] S. Watanabe and K. Miyake, *Origin of drastic change of Fermi surface and transport anomalies in CeRhIn_5 under pressure*, J. Phys. Soc. Jpn. **79** (2010) p.033707.
- [76] S. Watanabe and K. Miyake, *Roles of critical valence fluctuations in Ce- and Yb-based heavy fermion metals*, J. Phys.: Condens. Matter **23** (2011) p.094217; unpublished.
- [77] Q. Si, S. Rabello, K. Ingersent, and J. L. Smith, *Locally critical quantum phase transitions in strongly correlated metals*, Nature **413** (2001) p.804.
- [78] P. Coleman C. Pépin, Q. Si, and R. Ramazashvili, *How do Fermi liquids get heavy and die?*, J. Phys.: Condens. Matter **13** (2001) p.R723.
- [79] Q. Si, *Global magnetic phase diagram and local quantum criticality in heavy fermion metals*, Physica B **378-380** (2006) 23.
- [80] It is noted that the order of the AF transition (as a consequence of $P_c \simeq P_v$) depend on the detail of the parameter set of the extended PAM and calculation scheme; S. Watanabe and K. Miyake, unpublished.
- [81] H. Shishido, R. Settai, D. Aoki, S. Ikeda, H. Nakawaki, N. Nakamura, T. Iizuka, Y. Inada, K. Sugiyama, T. Takeuchi, K. Kindo, T. C. Kobayashi, Y. Haga, H. Harima, Y. Aoki, T. Namiki, H. Sato, and Y. Ōnuki, *Fermi surface, magnetic and superconducting properties of LaRhIn_5 and CeTIn_5 (T: Co, Rh and Ir)*, J. Phys. Soc. Jpn. **71** (2002) p.162.
- [82] N. F. Phillips, R. A. Fisher, F. Bouquet, M. F. Hundley, P. G. Pagliuso, J. L. Sarrao, Z. Fisk, and J. D. Thompson, *Specific heat of CeRhIn_5 : the pressure-driven transition from antiferromagnetism to heavy-fermion superconductivity*, J. Phys.: Condens. Matter **15** (2003) p.S2095.
- [83] T. Muramatsu, N. Tateiwa, T. C. Kobayashi, K. Shimizu, K. Amaya, D. Aoki, H. Shishido, Y. Haga, and Y. Ōnuki, *Superconductivity of CeRhIn_5 under high pressure*, J. Phys. Soc. Jpn. **70** (2001) p.3362.
- [84] R. Settai, Y. Miyauchi, T. Takeuchi, F. Lévy, I. Sheikin, and Y. Ōnuki, *Huge upper critical field and electronic instability in pressure-induced superconductor CeIrSi_3 without inversion symmetry in the crystal structure*, J. Phys. Soc. Jpn. **77** (2008) p.073705.
- [85] T. Sugawara, N. Kimura, H. Aoki, F. Lévy, I. Sheikin, and T. Terashima, *Anomalous behavior of the upper-critical-field in heavy-fermion superconductor CeRhSi_3* , J. Phys. Soc. Jpn. **79** (2010) p.063701.
- [86] I. Sheikin, A. Huxley, D. Braithwaite, J.-P. Brison, S. Watanabe, K. Miyake, and J.

- Flouquet, *Anisotropy and pressure dependence of the upper critical field of the ferromagnetic superconductor UGe₂*, Phys. Rev. B **64** (2001) p.220503(R).
- [87] S. Watanabe and K. Miyake, *Coupled CDW and SDW fluctuations as an origin of anomalous properties of ferromagnetic superconductor UGe₂*, J. Phys. Soc. Jpn. **71** (2002) p.2489.